International Journal of VLSI System Design and Communication Systems

ISSN 2322-0929
Vol.01,Issue.01,
August-2013,
Pages:17-25

www.semargroups.org

A Super Resolution Image from Low Resolution Image through Bregman Iteration Using Morphological Operators

HIMANEE[2], KARTHIK[3]

[1]M.Tech, ECE Dept, NREC, Hyderabad, AP-India, Email: nvhimanee417@gmail.com,
[2]M.Tech, ECE Dept, NREC, Hyderabad, AP-India.

Abstract: Morphological operators are well known tool that can extract structure from image, which are used in image denoising, image segmentation and image fusion. In this paper we model a non linear regularization method based on multi scale morphology for edge preserving super resolution (SR) image reconstruction. We formulate SR reconstruction problem from low resolution (LR) image as a deblurring and denoising and then solve the inverse problem using Bregman iterations. The proposed algorithm can hold inherent noise generated during low-resolution image formation as well as during SR image estimation efficiently. The effectiveness of the proposed method and reconstruction method for SR image can observe in experimental results.

Keywords: morphological operators, Bregman iteration, deblurring, denoising, operators splitting, sub gradients.

I. INTRODUCTION

It is always desirable to generate a Super Resolution (SR) image as it shows more intricate details. However, available sensors have limitation in respect to their maximum resolution. Thus our basic goal is to develop an algorithm to enhance the spatial resolution of images captured by an image sensor with a fixed resolution. This process is named as SR method and has remained an active research topic for the last two decades. More fundamental assumptions are made about image formation and quality, which in turn lead to different SR algorithms. These assumptions include the type of motion, the type of blurring, and also the type of noise. It is also important whether to produce the very best HR image possible or an acceptable HR image as quickly as possible.

Moreover, SR algorithms may vary depending on whether only a single low-resolution (LR) image is available (single frame SR) or multiple LR images are available (multi frame SR).Also, SR image reconstruction algorithms work either: 1) in the frequency domain or 2) in the spatial domain. In this paper, we focus only on spatial domain approach for multi frame SR image reconstruction. Among spatial domain multi frame SR image reconstruction algorithms, delegate works include non uniform interpolation-based approaches [1], [2]. The advantage of these approaches is that their computational cost is relatively low, which makes them suitable for real-time applications. However, they do not consider the blur model or noise characteristics and hence quality of the reconstructed HR image is not good. Projections on a convex set based methods [3], [4]utilize the spatial domain observation model and incorporate some prior information. Though these methods are simple, their disadvantages are non uniqueness of solutions, slow convergence rate, and heavy computational cost. Iterative back projection based approaches [5] conduct SR reconstruction in a straightforward way.

However, they have no unique solution due to the ill-posed nature of the inverse problem, and difficult to choose some parameters. On the other hand, Bayesian maximum a posteriori (MAP) estimation based methods [1]–[3] explicitly use prior information in the form of a prior probability density on the HR image and provide a rigorous theoretical framework. In [3], an MAP-based joint formulation is proposed that combine motion estimation, segmentation, and SR together. Another class of SR reconstruction methods generate an HR image from a single LR image or frame. These methods are called “example-based SR”. These methods based on natural image edge prior [2], [4] or gradient profile prior [5]. Glasner et al. [1] merge the concepts of both single frame SR and multi frame SR for HR image reconstruction from a single frame. At present, SR image reconstruction algorithms with sparse image prior [3], [5] have been receiving more attention due to advancement of sparse coding techniques. Those algorithms are based on dual dictionary learning techniques on the pairs of LR and HR image patches.

The approach reported in this paper is based on the regularization framework, where the HR image is estimated based on some prior knowledge about the image (e.g., degree of smoothness) in the form of regularization. The probability-based MAP approach mentioned earlier is equivalent to the concept of regularization; only in this case it gives a probabilistic meaning to the regularization expression. Tikhonov regularization based on bounded variation (L2 norm) is one of the popular regularization methods for SR reconstruction. It imposes softness in reconstructed image, but at the same time some details loses (e.g., edges) in the present image.

The first successful edge preserving regularization method for de-noising and de-blurring is the total variance (TV) (L1norm) method. Another interesting algorithm, proposed by Farsiu et al in [2], employs bilateral total variation (BTV) regularization. To achieve further improvement, Li et al. [3] used a locally adaptive BTV (LABTV) operator for the regularization. Two other regularization terms were pro-posed recently for SR image reconstruction, named as “steering kernel degeneration” and “regularization” [4] . One of the restoration method SR of iterative image based on differentiable regularization terms with L p norm ($1 < p \leq 2$) use the gradient descent approach to obtain optimal solution. On the other hand, quite a few techniques[2]–[4] are available in the literature to efficiently handle non differentiable regularization terms with L1 norm (e.g., TV regularization).

A group of solvers, evolved from Bregman iteration [3], is one of recently developed methods for such non differentiable constraint optimization problems. Marquina and Osher [5] were first to use the Bregman iteration for fast SR image reconstruction with TV regularization. However, even though all these regularization terms for SR image reconstruction lead to a stable solution, their performance depends on optimization technique as well as regularization term. For example, with gradient descent optimization technique, the LABTV regularization outperforms BTV, which gives better result than TV regularization. On the other hand, based on TV regularization, Marquina and Osher obtained superior result by employing Bregman iteration. So we envisage that even better results would be obtained by combining Bregman iteration and a more sophisticated regularization method that can suppress noise in LR images and ringing artifacts occurred during capturing the details of the HR image.

We propose a new regularizing method based on multiscale morphologic operators and filters which are nonlinear in nature. Morphological operators and filters are well known tools that can extract structures from images .They are used in image denoising [2], [3], image segmentation [3], [4], and image fusion successfully. Since proposed morphologic regularization term uses non differentiable max and min operators, we develop an algorithm based on Bregman iterations and the forward–backward operator splitting using sub-gradients. It is seen that the results produced by the proposed regularization are less affected by a fore mentioned noise evolved during the iterative process.

The rest of this paper is organized as follows. In section II Low Resolution (LR) image formation model and inverse reconstruction of High Resolution (HR) image from multiple LR images. We introduce proposed multi-scale morphological operator regularizing method in Section III. In Section IV, we review Bregman iteration and develop an algorithm for SR image reconstruction with proposed morphological operators. Section V presents the experiment l results and compares our results with those of some existing regularization methods for SR image reconstruction. Finally, some concluding remarks are made in Section VI.

II.PROPOSED METHOD FOR SUPERRESOLUTION

In this paper, we implement an algorithm for reconstruction of a high resolution image using sp line interpolation and a set of low resolution images. The proposed algorithm categorized into three blocks. The first block is motion estimation and compensation (ME), the second one is sp line interpolation and final one is de-blurring (or) sharpening filter. The adaptive full search block matching algorithm is used for motion estimation (ME) and motion compensation (MC). Finally, reconstruct with cubic spline interpolation of HR image and de-blurring filter and the block diagram of proposed model as shown in the fig 1. According to proposed model the working procedure can be discussed as follows.

A. Full search motion estimation

Full search motion estimation algorithm [4] is used to compensate the local motion between two consecutive frames. By using the MAD (Mean Absolute Difference), the motion vectors of a current frame corresponding to the reference frame can be calculated is shown in bellow equation.

$$MAD = \frac{1}{mn}\sum_{x=0}^{m-1}\sum_{y=0}^{n-1}\left|r(x,y) - c(x,y)\right| \quad (1)$$

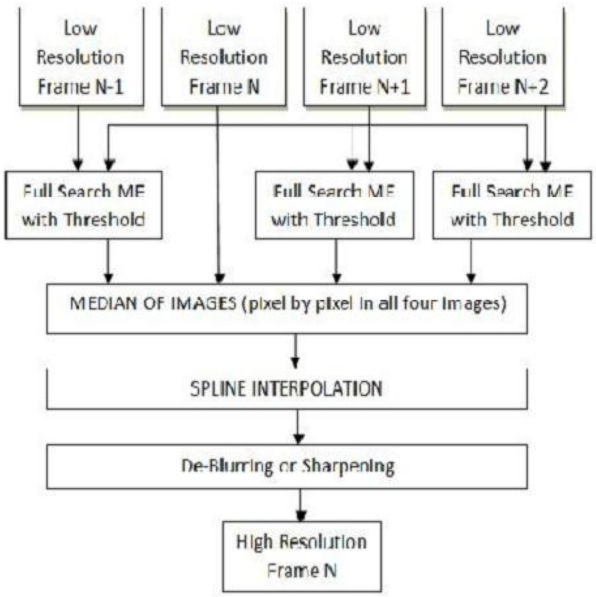

Fig.1. Proposed SR reconstruction model

Where r (x; y) is a reference frame and c (x; y) is a current frame. Finding a motion vectors using a full search algorithm is computational inefficient. In order to increase the performance of the algorithm and decreasing the number of computations, a full search algorithm is applied on Gray scale image and corresponding motion vectors are used on three R, G and B channels to compensate the sub-pixel motion between two consecutive frames. The number of computations further decreases by using threshold value. This threshold value can be calculated based on the estimation of the maximum motion between two consecutive frames. According to full search the MAD value is compared with threshold value and if MAD value is more than the threshold value the block is moved to next consecutive block. Due to threshold value some local error are occur in compensated image and these local error can be removed by finding the median image from the four compensated images. Median image is four frames combination and this is formed by finding a median of four pixel values at same location.

B. Cubic spline interpolation and de-blurring

Spline interpolation is a polynomial based interpolation in that each point on the polynomial is connected smoothly. We need a n+1 coefficients for each piece of polynomial of a degree n and first order spline is approximately equal to a linear interpolation. In a cubic interpolation the continuous and smooth spline curves are obtained from a series of unique polynomials between two data points. Cubic splines are used to determine the rate of change and cumulative changes over an interval. Cubic spline interpolation is used to interpolate the equally spaced and non-equally spaced data points. The spline is similar in principle. Numerical data are the points in this case. In these cubic polynomials weights are the coefficients used to interpolate the data and bend the line so that it passes through each of the data points without any breaks in continuity.

The main aim of the cubic spline interpolation is forming the interpolation formula at its boundaries within the interval [2]. The interpolation is continuous in the second derivative and smooth in the first derivative. The cubic interpolation of the interval x_j and x_{j+1} using in the tabulated function $R_i=R(x_i)$, i=1 ... N is given in bellow equation .

$$R = ER_j + FR_{j+1} + GR_j{}'' + AR_{j+1}{}''$$

The high resolution image constructed from a set low resolution images is shown in fig 1. Based on the method in fig 1 the motion compensated images obtained using full search motion estimation with threshold and find the median image using a three compensated fames and one original frame for decreasing the local error observed in a motion compensated images. Apply a cubic spline interpolation on median image to obtain a high resolution image. Due to spline interpolation the high resolution image losses some of the high frequency components. To recover the edges de-blurring or sharpening technique (unsharpened masking) is integrating with Spline Interpolation.

III. PROBLEM FORMULATION

The observed images of a scene are usually degraded by blurring due to atmospheric turbulence and inappropriate camera settings. The LR images are further degraded because of down sampling by a factor determined by the intrinsic camera parameters. The relationship between the LR images and the HR image can be formulated as [3].

$$Y_k = DF_kH_kX + e_k, \quad \forall k = 1, 2, ..., K \tag{1}$$

where Y_k , X, and e_k represent lexicographically ordered column vectors of the k^{th} LR image of size M, HR image of size N and additive noise, respectively. Geometric warp matrix is F_k and the blurring matrix H_k of size N×N incorporating camera lens/CCD blurring as well as atmospheric blurring. D is the down sampling matrix of size M × N and k is the index of LR images. Assuming that these images are taken under the same environmental condition and using same sensor, H_k becomes the same for all k and may be denoted simply by H. As a result, the LR images are related to the HR image as

$$Y_k = DF_kHX + e_k, \quad \forall k = 1, 2, ..., K. \tag{2}$$

Since under our assumption, D and H are the same for all LR images, we avoid down sampling and then up sampling at each iteration of iterative reconstruction algorithm by merging the up sampled and shifted-back LR images Y_k together. After applying up sampling and reverse shifting, Y_k will be aligned with HR image X. Suppose Y_k denotes the up sampled and reverse-shifted k^{th} LR image obtained through reverse effect of DFK of (2). That means $\underline{Y}_k = F_k^{-1} D^T Y_k$, where is the up sampling operator matrix

of size N × M and is an N × N matrix that shifts back (reverse effect of F^k) the image. Thus from (2) we can write

$$F_k^{-1} D^T Y_k = F_k^{-1} D^T D F_k H X + F_k^{-1} D^T e_k, \quad \forall k = 1, 2, \ldots, K$$
$$\text{i.e., } \underline{Y}_k = R_k H X + \underline{e}_k, \quad \forall k = 1, 2, \ldots, K$$

Where $R_k = F_k^{-1} D^T D F_k$ captures the contribution of pixels of the blurred image HX from which the LR image Y_k is generated. In our formulation, we have chosen purely integer valued translational shifts with respect to the HR grid. In that case, Fk has only 0 and 1 entries. Since D is just a down sample matrix applied on F_k , R_k has only 0 and 1 entries. For a more general formulation, if we incorporate rotational shifts as well in our motion model and/or if we use bilinear interpolation for non integer translational shift, R_k has real entries in the range [0, 1] and we may call it a weight matrix. However, in this paper we assume a purely integer-valued translational shift and R_k is called an index matrix.

Now, suppose Y is obtained by assembling all the available Y_k into a single HR grid [as shown in Fig. 1(b)], i.e., Y = $\sum_1^k \underline{Y}_k$ and $R = \sum_1^k R_k$. The relation between the HR and LR images can be rewritten as

$$Y = RHX + e. \qquad (3)$$

Note that the final index matrix R is similar to the transformation matrix derived in [3] except for the blurring term. Now, we get Y as a blurred image of actual HR image X except that some pixel values may be missing if we take fewer LR images, and index matrix R keeps track of those missing values. The unknown elements of Y can't participate in estimating X.

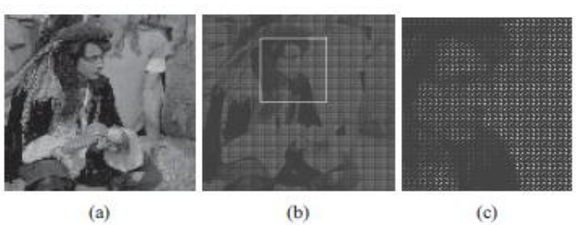

Fig. 2.Up sampling from LR images. (a) One of the four LR Images with down sampling factor 5. (b) Combined all four up sampled LR images with the corresponding pixel shifts and (c) cropped portion of the up-sampled image (b).

Suggested by (3). Fig. 2(a) shows one of four LR images Y_k (i.e., k = 1, 2, 3, 4) with a resolution factor 5 with different pixel shifts. Fig. 2(b) and (c) shows the corresponding Y and its cropped portion.

A. L2 Error-Based Estimation Of The Sr Image:

Since number of unknowns (pixels in the HR grid) in X is usually very large, a solution of (3) to obtain X by inversion of RH may not be feasible. Instead, we estimate an HR image Xˆ , which when degraded minimizes ρ(R H X, Y), i.e., Xˆ = arg min X ρ(R H X, Y) , where the dissimilarity measure ρ defined as $\rho(U, V) = (1/p)\|U - V\|_p^p, \ (1 \le p \le 2)$. .here we choose p = 2; then the estimated HR image satisfies (3)in the least-squares sense

$$\hat{x} = \arg \min_x \left[\left\| \left(rhx - \underline{y} \right) \right\| \frac{2}{2} \right] \qquad (4)$$

When K < N/M, the SR image reconstruction (4) becomes an ill-posed problem and, therefore, it becomes necessary to impose regularization to obtain a stable solution.

B. Regularization For The Sr Reconstruction Algorithm:

Regularization has already been used in conjunction with iterative methods for the restoration of noisy degraded images[2], [3], [5] in order to solve an ill-posed problem and prevent over fitting. To obtain a stable solution of (4),suppose that a regularization operator ϒ(X) in corporation prior knowledge is imposed on the estimated HR image X. The SR image reconstruction can simply be formulated as

$$\hat{X} = \arg\min\{\Upsilon(X) \ : \ \|RHX - \underline{Y}\|_2^2 < \eta\} \qquad (5)$$

where η is a scalar constant depending on the noise variance in the LR images. Now the constrained minimization problem of (5) may be reformulated as a unconstrained minimization problem as

$$\hat{X} = \arg\min_X \left\{ \frac{1}{2} \|RHX - \underline{Y}\|_2^2 + \mu \Upsilon(X) \right\} \qquad (6)$$

where μ is the regularization parameter that controls the emphasis between the data error term (first term) and the regularization term (second term). The selection of regularization parameter μ for optimum solution of (6) is a nontrivial task. For example, a large value of μ may not satisfy the constraint in (5) as the data error term is less emphasized; on the other hand, a small value of μ may amplify unwanted ringing artifacts as the smoothness criteria get less importance. One of the commonly used regularization methods is the Tikhonov cost function [1], [3], [4] for estimating stable de-noised image and is given by

$$\gamma(x) = \|\Gamma x\|2 \qquad (7)$$

where Γ is usually a high-pass operator such as derivative or Laplacian. Since high-pass operators enhance both the edges and noise equally, minimization of leads to blurring of edges along with the removal of noise. The first successful edge-preserving regularization method for denoising and de-blurring is the TV method [1], which penalizes the spatial variation in the image as measured by the L1 norm of the magnitude of the gradient

$$\gamma(x) = \|\Gamma x\|1 \qquad (8)$$

Often this is also called the Rudin–Osher–Fatemi model. Farsi et al. [2] introduced the BTV method by combining the total variation and the bilateral filter as follows:

$$\gamma(x) = \sum_{l=-w}^{w} \sum_{m=-w}^{w} \alpha^{|m|+|l|} \left| x - s_x^l s_x^l \right| \qquad (9)$$

Where l + m ≥ 0 and are the shift operator matrices to represent l and m pixel shifts, respectively, along the horizontal and vertical direction. w is a parameter, it estimates the window size, and α (0 < α < 1) is the weighting coefficient. The amount of edge sharpness preservation as well as the degree of smoothness depends on the value of α and w. Thus conventional regularization methods choose ϒ(X) as the high-frequency energy and minimize its p^{th} norm to ensure smoothness. In this paper, we define ϒ(X) based on morphologic filters that preserve structures and suppress noise. It is well known that morphological opening and closing remove bright and dark noise, without affecting the edge sharpness. An image, in general, may contain both detail and noise at different scales.

IV. MORPHOLOGICAL OPERATORS REGULARIZING

Let B be a disk of unit size with origin at its center and sB be a disk structuring element (SE) of size s. The morphological dilation Ds (X) of an image X of size m ×n at scale s is defined as

$$D_s(\mathrm{X}) = \begin{pmatrix} \max_{r\in(sB)_{(1)}}\{x_r\} \\ \max_{r\in(sB)_{(2)}}\{x_r\} \\ \ddots \\ \max_{r\in(sB)_{(mn)}}\{x_r\} \end{pmatrix}$$

Where D is a set of pixels covered under SE sB translated to the i^{th} pixel xi. Similarly, the morphological erosion Es(X) at scale s is defined as

$$E_s(\mathrm{X}) = \begin{pmatrix} \min_{r\in(sB)_{(1)}}\{x_r\} \\ \min_{r\in(sB)_{(2)}}\{x_r\} \\ \ddots \\ \min_{r\in(sB)_{(mn)}}\{x_r\} \end{pmatrix}.$$

Morphological opening Os (X) and closing Cs (X) by SE sB are defined as follows:

Os (X) = Ds (Es(X))

Cs (X) = Es(Ds (X))

In multi-scale morphological image analysis, we have seen that the difference between the s^{th} scale closing and opening extracts noise particles and image artifacts in scale s and may be used for de-noising purposes. So in this paper, we propose the regularization function based on multi-scale morphology as

$$\Upsilon(\mathrm{X}) = \sum_{s=1}^{S} \alpha^s \mathbf{1}^t [C_s(\mathrm{X}) - O_s(\mathrm{X})] \qquad (10)$$

Where 1 is a column vector consisting of all 1s and α is the weighting coefficient. To give more emphasis on the small scale for noise removal, the value of α is chosen from 0 < α < 1. Therefore, the proposed regularization term, the SR reconstruction problem (5) is reduced to

$$\hat{\mathrm{X}} = \min_{\mathrm{X}} \left\{ \sum_{s=1}^{S} \alpha^s \mathbf{1}^t [C_s(\mathrm{X}) - O_s(\mathrm{X})] : \|RH\mathrm{X} - \underline{\mathrm{Y}}\|_2 < \eta \right\}. \qquad (11)$$

V. SUBGRADIENT METHODS AND BREGMAN ITERATION

Bregman iteration was successfully used by Osher et al. [2] in the field of computer vision for finding the optimal value of energy functions in the form of a constrained convex functional. Since then, a class of efficient solvers has been proposed for constrained (5) and unconstrained problems (6). Among them, the “fixed point continuation” (FPC) [2] method was proposed to solve the unconstrained problem by performing gradient descent steps iteratively. The linearized Bregman algorithm [4] is derived by combining the FPC and Bregman iteration to solve the constrained problem in a more flexible ways. These methods are successfully used in sparse reconstruction problem, i.e., compressed sensing [1], [3] and sparse coding [2], [4]–[5], due to their simplicity, efficiency. Later, Goldstein et al developed the “split Bregman method” for more structured regularization in variational problems of image processing. Marquina and Osher formulated a model for SR based on a constrained variational model that uses the total variation of the signal as a regularizing functional. In this section, we develop an algorithm based on Bregman iteration and the proposed morphologic regularization for the SR image reconstruction problem.

A.Bregman Iteration

Consider the following minimiz problem:

$$\min_{\mathrm{X}} \{\Upsilon(\mathrm{X}) \ : \ T(\mathrm{X}) = 0\} \qquad (12)$$

Where X and T are both convex functional defined over, $\mathbb{R}^n \rightarrow \mathbb{R}^+$ Now the Bregman iterations that solve the above constrained minimization problem are as follows:

Initialize $\mathbf{X}^0 = p^0 = \mathbf{0}$

$$\begin{cases} \mathbf{X}^{(n+1)} = \arg\min_{\mathbf{X}} \{\mu B_\Upsilon^{p^{(n)}}(\mathbf{X}, \mathbf{X}^{(n)}) + T(\mathbf{X})\} \\ p^{(n+1)} = p^{(n)} - \nabla T(\mathbf{X}^{(n+1)}) \end{cases} \quad (13)$$

where $B_\Upsilon^{p^{(n)}}$ is the Bregman distance corresponding to convex functional $\Upsilon(.)$ and is defined from point X to point V as $B_\Upsilon^p(\mathbf{X},\mathbf{V}) = \Upsilon(\mathbf{X}) - \Upsilon(\mathbf{V}) - \langle p, \mathbf{X} - \mathbf{V} \rangle$.Convergence and stability of this scheme are discussed in detail in [2]. Yin et al. [4] have shown that for the case of linear constraints $RH\mathbf{X} - \underline{\mathbf{Y}} = 0$ in, Bregman iterations can be reduced to a more simplified form [5] with l2 norm

$$\begin{cases} \mathbf{X}^{(n+1)} = \arg\min_{\mathbf{X}} \{\mu \Upsilon(\mathbf{X}) + \frac{1}{2}\|RH\mathbf{X} - \mathbf{Y}^{(n)}\|_2^2\} \\ \mathbf{Y}^{(n+1)} = \mathbf{Y}^{(n)} + (\underline{\mathbf{Y}} - RH\mathbf{X}^{(n+1)}) \end{cases} \quad (14)$$

In other words the error (Y RHX $^{(n)}$) in nth estimation is added back to Y(n) such that finally RHX$^{(n)}$ satisfies the constraint RHX Y = 0. Note that the first equation solves the unconstrained minimization problem. In general, there is no explicit expression for X$^{(n+1)}$ to solve the unconstrained optimization sub-problem (first equation) (14), we go further to solve it explicitly.

B.Proximal Map:

Consider the following unrestrained maximize problem:

$$\min_{\mathbf{X}} (\mu \Upsilon(\mathbf{X}) + T(\mathbf{X})) \quad (15)$$

where μ > 0. Combettes et al. [5] describe a forward–backward technique to minimize the sum of two convex functionals based on the proximal operator introduced by Moreau [2]. By classical arguments of convex analysis, the solution of (16) satisfies the condition

$$\mu \partial \Upsilon(\mathbf{X}) + \partial T(\mathbf{X}) = 0.$$

For any positive number γ, we have

$(X + \gamma\mu\partial\Upsilon(\mathbf{X})) - (X - \gamma\, \partial T(X)) = 0$.

This leads to onward and toward the back splitting algorithm

$X(k+1) = \mathrm{Prox}\Upsilon(X(k) - \gamma\, \partial T(X(k)))$ (14)

where Prox is the proximal operator Proxϒ(V) is defined as

$$\mathrm{Prox}_\Upsilon(\mathbf{V}) = \arg\min_{\mathbf{X}} \left\{\mu\Upsilon(\mathbf{X}) + \frac{1}{2\gamma}\|\mathbf{X} - \mathbf{V}\|_2^2\right\}. \quad (16)$$

In our case, $T(\mathbf{X}) = (1/2)\|RH\mathbf{X} - \underline{\mathbf{Y}}\|_2^2$, Therefore, the solution of the minimization problem (16) can be computed by the following two-step algorithm:

$$\begin{cases} \mathbf{U}^{(k+1)} = \mathbf{X}^{(k)} - \gamma H^T R^T (RH\mathbf{X}^{(k)} - \underline{\mathbf{Y}}) \\ \mathbf{X}^{(k+1)} = \arg\min_{\mathbf{X}} \left\{\mu\Upsilon(\mathbf{X}) + \frac{1}{2\gamma}\|\mathbf{X} - \mathbf{U}^{(k+1)}\|_2^2\right\}. \end{cases} \quad (17)$$

This algorithm (16) can be used to solve the unconstrained minimization problem presented by the first equation of (15) as described next.

C. Bregmanized Operator Splitting

In this section, we develop an algorithm to solve the equality-constrained minimization problem (14) with T (X):=RHX−Y using Bregman iterations (15) and operator splitting (18), briefly introduced in the last two subsections. Now, the operator splitting technique is used to solve the unconstrained sub problem, i.e., first equation of (15), as follows: for k ≥ 0, X (n+1, 0) = X(n)

$$\begin{cases} U^{(n+1,\,k+1)} = \mathbf{X}^{(n,\,k)} - \gamma H^T R^T (RH\mathbf{X}^{(n,\,k)} - \mathbf{Y}^{(n,\,k)}) \\ \mathbf{X}^{(n+1,\,k+1)} = \arg\min_{\mathbf{X}} \left\{\mu\Upsilon(\mathbf{X}) + \frac{1}{2\gamma}\|\mathbf{X} - U^{(n+1,\,k+1)}\|_2^2\right\} \end{cases} \quad (18)$$

Ideally, we need to iterate (19) infinite number of times [5] to obtain a convergent solution $\mathbf{X}^{(n+1)}$ for the said sub problem. Instead, we propose to iterate them once for small amount of noise, which leads to the following algorithm:

$$\begin{cases} \mathbf{U}^{(n+1)} = \mathbf{X}^{(n)} - \gamma H^T R^T (RH\mathbf{X}^{(n)} - \mathbf{Y}^n) \\ \mathbf{X}^{(n+1)} = \arg\min_{\mathbf{X}} \left\{\mu\Upsilon(\mathbf{X}) + \frac{1}{2\gamma}\|\mathbf{X} - \mathbf{U}^{(n+1)}\|_2^2\right\} \\ \mathbf{Y}^{(n+1)} = \mathbf{Y}^{(n)} + (\underline{\mathbf{Y}} - RH\mathbf{X}^{(n+1)}). \end{cases} \quad (19)$$

Proposed Iterative Algorithm for super resolution Image: Initialize Y(0) = n = 0;Y, X (0) = FillUnknown(Y);

While

$$(\|RH\mathbf{X}^{(n)} - \underline{\mathbf{Y}}\|_2^2 > \eta)$$

$$\begin{cases} \mathbf{U}^{(n+1)} = \mathbf{X}^{(\tilde{n})} - \gamma H^T R^T (RH\mathbf{X}^{(n)} - \mathbf{Y}^n) \\ \mathbf{X}^{(n+1)} = \mathbf{U}^{(n+1)} - \mu' \left| \frac{\delta\Upsilon(\mathbf{X})}{\delta\mathbf{X}} \right|_{\mathbf{X}^{(n)}} \\ \mathbf{Y}^{(n+1)} = \mathbf{Y}^{(n)} + (\underline{\mathbf{Y}} - RH\mathbf{X}^{(n+1)}) \end{cases}$$

$$n = n + 1 \quad (20)$$

End

FillUnknown (Y) in the initialization step of the above algorithm fills the unknown pixels in Y by the corresponding known neighboring pixels. The parameter h is a predefined threshold chosen depending on variance of noise in LR images and significantly small for noise-free LR images. So we iterate until constraint in (5) is satisfied.

Note that, for LR images with high noise to satisfy in-equality constraint in (5), a fraction b (where b < 1) of the error (Y RHX $^{(n)}$) in n-th estimation is added back to Y $^{(n)}$, i.e. last equation of (IV.10) is replaced by $Y^{(n+1)}=Y^{(n)}+ b\,(Y\; RHX^{(n+1)})$ and is iterated once after every literations of first two equation. Since proposed regularization function $\Upsilon(\mathbf{X})$ as defined in equn. (10) consists of non-differentiable max and min operators (D_s (X); E_s (X)), we go for computing sub-gradients $\left|\frac{\delta\Upsilon(\mathbf{X})}{\delta\mathbf{X}}\right|_{\mathbf{X}(n)}$ of the morphological regularization $\Upsilon(\mathbf{X})$ in the following subsection.

D. Subgradients Of Morphologic Regularization Function

Here we derive the sub gradients of the dilated (10) and eroded (11) image with respect to its pixel values. Let us denote the sub gradient of a dilated image Ds (X) by δDs / δX. From the definition of Ds (X), as given in (10), the j th element of the ith column of the sub-gradient (δDs/δX) is

$$\frac{\delta D_{s,j}}{\delta x_i} = \begin{cases} 1, & \text{if } x_i = \max_{r\in(sB)_{(j)}}\{x_r\} \text{ and} \\ & \forall t \in (sB)_{(j)}, t \neq i, x_t < x_i \\ 0, & \text{if } x_i < \max_{r\in(sB)_{(j)}}\{x_r\} \\ \in [0,1], & \text{elsewhere.} \end{cases} \quad (21)$$

Similarly, the sub-gradient of an eroded image Es (X) can be written as follows:

$$\frac{\delta E_{s,j}}{\delta x_i} = \begin{cases} 1, & \text{if } x_i = \min_{r\in(sB)_{(j)}}\{x_r\} \text{ and} \\ & \forall t \in (sB)_{(j)}, t \neq i, x_t > x_i \\ 0, & \text{if } x_i > \min_{r\in(sB)_{(j)}}\{x_r\} \\ \in [0,1], & \text{elsewhere.} \end{cases} \quad (22)$$

Now, in (21) and (22) we choose the sub-gradient equal to 1 out of the range [0, 1]. The sub gradients become

$$\frac{\delta D_{s,j}}{\delta x_i} = \begin{cases} 1, & \text{if } x_i = \max_{r\in(sB)_{(j)}}\{x_r\} \\ 0, & \text{if } x_i < \max_{r\in(sB)_{(j)}}\{x_r\} \end{cases} \quad (23)$$

$$\frac{\delta E_{s,j}}{\delta x_i} = \begin{cases} 1, & \text{if } x_i = \min_{r\in(sB)_{(j)}}\{x_r\} \\ 0, & \text{if } x_i > \min_{r\in(sB)_{(j)}}\{x_r\}. \end{cases} \quad (24)$$

Since an analogous chain rule holds for the sub gradients,(23 and 24) we can write down the sub gradients of the regularization function.

VI. RESULTS AND DISCUSSION

In this section, we study and analyze the performance of the proposed method as well as that of some other existing SR reconstruction methods. In this discussion, the proposed algorithm (22) is referred to as "Breg+ Morph," while the other methods are referred to as "Grd + TV" [1], "Grd +BTV" [2], "Breg + TV" [3], and "Grd + LABTV" [1],respectively. Here, "Grd" stands for iterative gradient descent technique and "Breg" stands for Bregman iteration technique for optimization. "Morph," "TV," "BTV"these are all stand for morphological, total variation, BTV respectively. We note that these methods associated with "Breg" solve constrained SR reconstruction formulation (5),whereas those with "Grd" solve the unconstrained formulation (6).Experimental Setting: For performance evaluation, a typical512 × 512 gray-level HR image (e.g., Chart image) is chosen[see Fig. 2(a)]. We synthetically generate some LR images from this HR image and later reconstruct an HR image from these generated LR images. Finally, we compute the peak signal-to-noise ratio (PSNR) and SSIM as the quantitative measures of quality of reconstructed HR image with respect to the original HR image. The blurring is chosen as a 5 × 5Gaussian smoothing kernel with scale parameter σ = 2.5, and according to the matrix H is formed. The downs ampling factor

TABLE: 1
TIME COMPARISON OF DIFFERENT METHODS IN FIGURE 3.

method	TV	BTV	Breg+morph
iterations	221	211	6

Method Grd + TV Grd + BTV Breg + Morph is chosen to be 5 and the matrix D is constructed to achieve this. We assume purely translational shifts by the integer value and F_k is formed accordingly. There are 25 possible choices of integer shifts for the resolution factor 5 to generate 25LR images. In our experiment, we have observed that only10 LR images among 25 are sufficient to reconstruct HR image of acceptable quality with resolution factor 5. Hence, in our experiment we take 10 randomly chosen LR images and determine the index matrix R of (3) accordingly. The same setup is followed throughout this experimental section unless stated otherwise. Second, an interesting portion is marked on each resultant HR image and is displayed on the top-right/left corner after zooming it for careful study of the visual quality. The parameters for each algorithm are chosen to maximize the PSNR with respect to the ground truth. In our reconstruction algorithm (22), we have chosen the model parameters γ = 1and μ = 0.5 and have got good results in most of the experiments. To experiment with the noisy LR images, for every five iterations of the first two steps of the algorithm(22) the third step is executed once and β is chosen as the reciprocal of the noise variance. We have implemented the algorithms using MAT-LAB 7.6 and run in Desktop with a 3-GHz Intel quad-core processor and 8 GB of RAM. In the first experiment, the LR images contain small amounts of noise (σ = 2), and the up sampled and merged image obtained from 10 LR images.

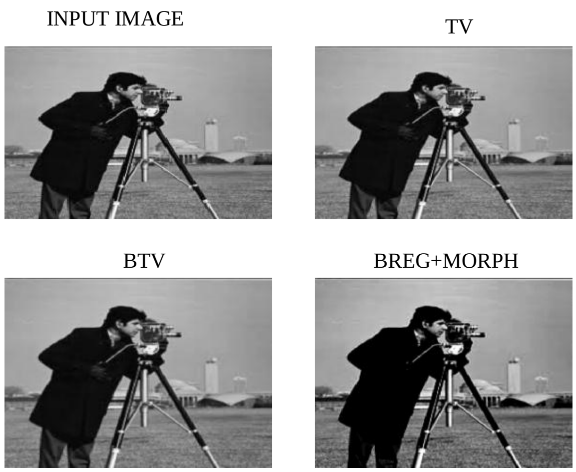

Fig3. Simulation Results.

The results of different algorithms are shown in Fig. 3(d)–(h).Fig. 3(d)–(f) present SR reconstructed images using gradient descent method for optimization with TV, BTV, and LABTV regularizations, respectively. Similarly Fig. 2 present the results using Bregman iteration method for optimization with TV and morphologic regularizations, respectively. In each case, the algorithm is terminated if the residue is less than a certain threshold [e.g., η in the algorithm (22)] or number of iterations is more than 1000. Table I shows the number of iterations, and Fig. 4 show the corresponding numerical time comparison of the results. It is seen that the morphologic regularization yields SR reconstructed image of better quality compared to other regularization methods with less number of iterations.

In Section IV-A, it was mentioned that the convergence and stability of the Bregman iteration based scheme are discussed in detail in [2] and [5]. However, here we give an indication of the same based on experimental data. For this purpose, in Fig. 4(b) we plot the objective function of Breg + TV, Breg + BTV and Breg + Morph up to the number of iterations as given in Table I. This figure shows that, after initial irregularities, the values of the objective function show an overall a decrease. (a) Illustrates how residue of data fidelity term approaches the threshold value to terminate the algorithm IV-A, (b) variation in objective function with iteration for 'Breg+TV' and 'Breg+Morph'[see text] and (c) PSNR up to 100 iterations for different algorithms as indicated in (a). Actual number of iterations and run time are shown in Table I.

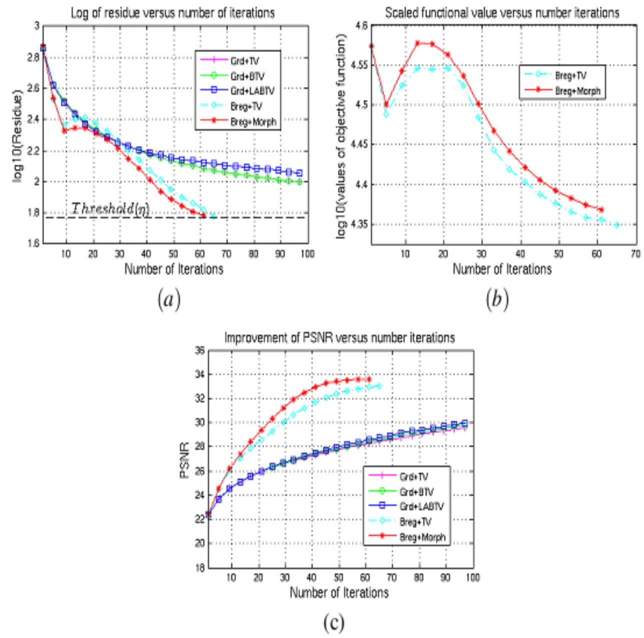

Fig.4.Comparison of reconstruction qualities of different methods versus number of iterations for the experiment in figure 3.

VII.CONCLUSION

In this paper, we have presented an edge-preserving SR image reconstruction problem as a de-blurring problem with a new robust morphologic regularization method. Here we put forward two major contributions. First, we proposed a morphologic regularization function based on multi-scale opening and closing, which could remove noise efficiently while preserving edge information. Secondly, we employed Bregman iteration method to solve the inverse problem for SR reconstruction with the proposed morphologic regularization. It is well known that multi-scale morphological filtering can reduce noise efficiently, so we have built up successfully a regularization method based on multi-scale morphology.

Our experimental section shows that it works quite well, in fact better than existing methods. Nonlinearity of the regularization function is handled in a linear fashion during optimization by means of the sub gradient and proximal map concept. We also showed that, if there is impulse noise with random values or salt-and-pepper noise in LR images, they can be handled efficiently using our two-step SR reconstruction algorithm. It first detects the noisy pixels (note: it does not substitute their values) and then, by considering those detected pixels as unknown pixels, reconstructs SR image using only those pixels which are not corrupted by noise. The morphologic regularization method proposed here was tested only on SR reconstruction problem, but one can easily extend this method to other ill-posed problems as well. Also, one can

extend this regularization method to be adaptive by choosing SE of different shapes and sizes depending on the local statistics of neighboring pixels. We can extend this project by increasing the peak signal to noise ratio and mean square error for an output image by using more morphological operations so that to decrease the noise by edge preserving and decreasing the number of iterations by using the wavelets transforms so as to increase the efficiency.

VIII. REFERENCES

[[1] S. Lertrattanapanich and N. K. Bose, "High resolution image formation from low resolution frames using Delaunay triangulation.

[2] N. Nguyen and P. Milanfar, "An efficient wavelet-based algorithm for image super resolution".

[3] H. Stark and P. Oskoui, "High resolution image recovery from image plane arrays, using the convex projections".

[4] A. J. Patti and J. Altunk, "Artifact image reconstruction with edge adaptive constraints and higher-order interpolants,".

[5] M. Irani and S. Peleg, "Improving resolution by image registration".